

## Colloidal Silver Nanoparticles Synthesized by Chemical Reduction Method

V. SUMAN<sup>a,b,\*</sup>, M. RUSU<sup>c</sup> AND L. GHIMPU<sup>b</sup>

<sup>a</sup>Doctoral School "Natural Sciences", Moldova State University, Alexei Mateevici St 60, MD-2009, Chisinau, Republic of Moldova

<sup>b</sup>Institute of Electronic Engineering and Nanotechnologies, Technical University of Moldova, Academy St 3/3, MD-2028, Chisinau, Republic of Moldova

<sup>c</sup>Institute of Chemistry, Moldova State University, Academy St 3, MD-2028, Chisinau, Republic of Moldova

Doi: [10.12693/APhysPolA.146.446](https://doi.org/10.12693/APhysPolA.146.446)

\*e-mail: [victor.suman@iien.utm.md](mailto:victor.suman@iien.utm.md)

Silver nanoparticles were prepared by chemical reduction method. Silver nitrate was taken as a metal precursor, chondroitin sulfate as a stabilizing agent, and glucose as a reducing agent. The formation of Ag nanoparticles was monitored using ultraviolet-visible absorption spectroscopy, X-ray diffraction, and Fourier-transform infrared spectroscopy. X-ray diffraction analysis confirmed the presence of elemental Ag signal, with no peaks of other impurities detected. The ultraviolet-visible spectra of colloidal solutions of Ag nanoparticles show that the chondroitin sulfate concentration has a substantial influence on the reaction rate of Ag nanoparticle formation, as well as on the size of the nanoparticles. The position and shape of plasmonic absorption spectra of Ag nanoparticles also depend on the duration of the synthesis reaction. Functional groups identified with Fourier-transform infrared spectroscopy confirm the formation of high-purity Ag nanoparticles.

topics: chemical reduction method, Fourier-transform infrared spectroscopy (FTIR), ultraviolet-visible (UV-Vis), X-ray diffraction (XRD)

### 1. Introduction

Silver nanoparticles (AgNPs) are among the widely investigated nanoparticles due to their unique electrical, optical, magnetic, mechanical, and chemical properties that depend on their size and shape, and make them extremely important for their potential in technological applications. For this reason, current research on nanostructured materials is devoted mainly to understanding changes in the fundamental properties of matter at the nanoscale. The study of the mechanisms involved in the process of nanoparticle formation and growth is of fundamental importance to understanding the chemical process and controlling the microstructure development of nanoparticles.

The application of modern spectroscopic techniques to study the microstructural evolution of metallic microclusters plays a major role in the chemistry of these materials, as it provides the possibility to monitor *in situ* new reaction schemes for the synthesis of nanometric clusters. Another important point concerns the reproducibility of the microclast formation and growth process. Since the properties of nanostructured materials are strictly

related to their microstructure (i.e., shape, size, and composition), it is very important to know the influence of different experimental conditions on the synthesis process in order to enable the reproducibility of the reaction. The syntheses can be classified as "green" and "non-green." The "green" approach involves the use of environmental agents such as tannins, saccharides, and plant extract necessary for the formation and stabilization of nanoparticles. The main advantages of plant-based biological systems, such as nanoparticle production, are low cost of cultivation, low synthesis time of the final product, and biological safety of the product. Recently, biological methods of the synthesis of nanoparticles (biosynthesis) have become increasingly widespread. Biological methods include synthesis using micro-organisms. A whole series of nanoparticles have been obtained in this way, e.g., AuNPs, AgNPs, CdSNPs, etc. [1]. This "green" approach to the synthesis of AgNPs is quite innovative and offers a valuable contribution to the field of materials for patterned and structural electronics [2].

Metal nanoparticles have a high surface area, strong adsorption, and high reducibility and can be used in biomedical applications, including antibacterial, anticancer, antioxidant, and drug

delivery mechanisms [3]. The chemical reduction method for the synthesis of AgNPs involves working with reagents containing the appropriate Ag salt, a reducing agent, and a stabilizing agent. The surface morphology of the resulting nanomaterial is governed by the nature of the stabilizing agent, the molar ratio of the reducing agent to silver salt, the oxidation–reduction potential, the solvent stirring, the synthesis rate, and temperature. Among all the above-mentioned parameters, the stabilizer concentration for the production of AgNPs is essential. The use of  $\text{AgNO}_3$  increases the possibility that  $\text{NO}_3$  is the dominant anion associated with the silver nanomaterial. The reducing agent can be any chemical agent, plant extract, or biological agent, such as  $\text{H}_2$ , gas, sodium borohydrin, hydrazine, ethanol, ethylene glycol, or ascorbic acid [4]. The simplest and most commonly used method for the synthesis of metal nanoparticles in bulk solution is the chemical reduction of metal salts [5]. In fact, the production of nanometric metallic silver particles with different morphologies and sizes has been reported [6] using chemical reduction of silver salts [7]. This synthetic method involves the reduction of an ionic salt in a suitable medium in the presence of a surfactant using various reducing agents [8].

In this work, a methodology was developed to evaluate the growth of silver nanoparticles during their formation in the chondroitin–glucose– $\text{AgNO}_3$  system using the chemical reduction of silver nitrate.

## 2. Materials and methods

### 2.1. Materials

Chondroitin sulfate (ChS) was purchased from Merck (Sigma-Aldrich) with a purity of 99%, glucose was purchased from POCH S. A. (Poland) with a molar mass of 40000, and  $\text{AgNO}_3$  was also purchased from Merck (Sigma-Aldrich) with a purity of 99.99%.

### 2.2. “Green” synthesis of chondroitin-coated AgNPs

Chondroitin sulfate (ChS) has been used as a coating agent due to its excellent biocompatibility and biodegradability. ChS is an anionic polyelectrolyte with negatively charged sulfate and carboxylate groups. The procedure for synthesizing silver nanoparticles (AgNPs) using ChS as a stabilizing agent and glucose as a reducing agent is relatively simple. In a typical preparation process, silver nitrate ( $\text{AgNO}_3$ ) solution was combined with ChS solution and glucose, and then the mixture was stirred at  $40^\circ\text{C}$ . In this method, double-distilled water was



Fig. 1. Colloidal silver solutions obtained by chemical reduction of  $\text{AgNO}_3$  using ChS and glucose. The numbering of colloidal solutions is: 11 — colloidal solution after 2 h from the beginning of infusion; 12 — after 4 h; 13 — after 6 h; 14 — after 12 h; 15 — after 24 h; 16 — after 30 h; 17 — after 48 h.

Conditions for the synthesis of AgNPs. TABLE I

No.	Temperature [ $^\circ$ ]	$C_M (\times 10^{-3})$ [M]		
		$\text{AgNO}_3$	ChS	Glucose
1	40	5.89	0.45	5.55
2	40	5.89	0.89	5.55
3	40	5.89	1.34	5.55
4	40	5.89	1.79	5.55
5	40	5.89	2.24	5.55
6	40	5.89	2.69	5.55

used as an environmentally friendly solvent. The reaction time for the reduction of  $\text{Ag}^+$  ions at  $40^\circ\text{C}$  was found to be essential to ensure complete reduction. The mixture was stirred continuously during the entire synthesis process using a magnetic stirrer. At predetermined time intervals, samples were taken from the reaction mixture to monitor surface plasmon resonance. The conditions used for the preparation of AgNPs are shown in Table I. There, the synthesis conditions, including the molar concentration of  $\text{AgNO}_3$ , ChS, and glucose, and the solution temperature throughout the synthesis are indicated.

While most of the reduction is completed at a higher ChS concentration, only a small fraction of  $\text{Ag}^+$  ions is reduced at an equimolar concentration. The overall shape of the plasmon absorbance remains constant, indicating that the overall particle distribution is not influenced by the concentration of ChS. The reduction of silver  $\text{Ag}^+$  ions using ChS was monitored by analyzing the changes in absorbance at different time intervals during the synthesis.

It is well known that silver ions are soluble in deionized water. Based on these results, it can be concluded that all silver ions have been removed. Sodium chloride was added to confirm the completeness of the reaction and to verify the complete transformation of the silver ions into silver nanoparticles (AgNPs). The appearance of opalescence (Fig. 1) in the reaction solution indicates the presence of silver

ions, while a clear solution confirms the completion of the reaction.

Excess unreacted ChS and the silver ions remaining in suspension were separated from the ChS–AgNPs nanoparticles using a sedimentation device by centrifugation at 3000 rpm for 10 min. At the end of the centrifugation process, the AgNPs sediment to the bottom of the vial, and the solution becomes transparent. Thus, the obtained AgNPs were purified initially with double-distilled water and then with a 50/50 solution of ethyl alcohol and acetone. Finally, AgNPs were dried in an oven at 40°C.

### 2.3. Investigation methods

The *ultraviolet-visible* (UV-Vis) spectra were recorded using the UV-Vis spectrophotometer Cary 300, utilizing a spectral range of 200–800 nm, deuterium and halogen light sources, and a photomultiplier detector for a spectral resolution of up to 0.1 nm and photometric accuracy of  $\pm 0.005$  Abs. The *Fourier-transform infrared spectroscopy* (FTIR) spectra were recorded at room temperature using the Bruker ALPHA spectrometer, in the wavelength range of 4000–400  $\text{cm}^{-1}$ , in the scientific research laboratory “Advanced Materials in Biopharmaceutics and Technics” of the State University of Moldova, Republic of Moldova.

## 3. Results and discussion

### 3.1. SEM morphology

The *scanning electron microscope* (SEM) images in Fig. 2 show the presence of well-dispersed particles that are more or less spherical, as well as some faceted particles. The size distribution shows a bimodal distribution of particle sizes, with the first group ranging from 20 to 40 nm and the second from 40 to 60 nm. Consequently, the shift of the surface plasmon absorption maximum from 464 to 471 nm (ChS concentration =  $0.89 \times 10^{-3}$  M) could be due to a difference in particle shape.

### 3.2. UV-VIS spectroscopy

The evolution of AgNPs was monitored using UV-VIS spectroscopy [9]. Figure 3 illustrates the UV-VIS absorption spectra of AgNPs at different reaction time intervals. The characteristic *surface plasmon resonance* (SPR) peak at about 456 nm observed at different reaction times confirmed the formation of AgNPs. During a longer reaction, from 2 to 48 h, the intensity of the SPR peak increased,

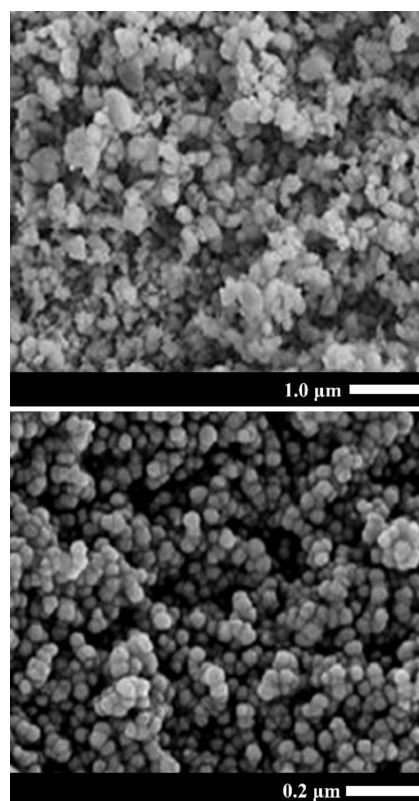


Fig. 2. SEM images of synthesized AgNPs.

accompanied by a slight redshift, but without a significant broadening of the peak. The increase in intensity indicated a higher concentration of AgNPs, while the small redshift of the SPR peak suggested a slight increase in particle size as the reaction progressed. To evaluate the effect of ChS concentration on the preparation of AgNPs, the reactions were carried out at different ChS/AgNO<sub>3</sub> mass ratios. Colloidal silver obtained at the lowest mass ratios showed a light red shade. As the mass ratios increased, the color of the solution gradually changed to red-brown, and the intensity of the SPR peak increased, as shown in Fig. 3.

The ChS concentration has a substantial influence on the reaction rate of AgNPs formation, as well as on the size of the nanoparticles themselves. In Fig. 4, we observe that the SPR absorption maximum is positioned at 454 nm for  $0.45 \times 10^{-3}$  M of ChS and shifts up to 473 nm for  $2.24 \times 10^{-3}$  M. After 48 h from the beginning of the synthesis, by comparing the curves in Fig. 3, we observe a shift of the absorption maxima from 454 nm for  $0.45 \times 10^{-3}$  M to 517 nm, which can be attributed to the increase in nanoparticle size, as well as the joining of other nanoparticles to the already formed clusters. The smallest shift of the absorption maxima was observed for ChS concentrations of  $0.89 \times 10^{-3}$  M from 464 to 471 nm, which suggests that with increasing synthesis duration the nanoparticle sizes, do not essentially change.

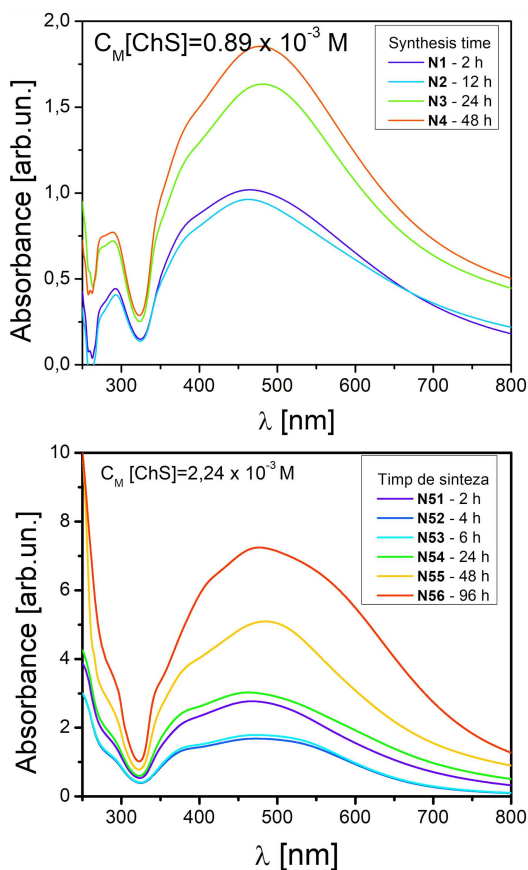


Fig. 3. UV-VIS spectra of colloidal solutions of AgNPs, obtained for different concentrations of ChS and different synthesis times.

The UV-VIS absorption spectra of silver nanoparticles dispersed in double-distilled water are shown in Fig. 5. The position and shape of the *plasmonic absorption spectrum* (SPAS) depend on the shape (spherical or nearly spherical) and size of the synthesized silver nanoparticles. This is consistent with the study by Mock et al. [10] that demonstrated a correlation between the shape and size (20–100 nm) of the synthesized silver nanoparticles. Silver nanoparticles synthesized in the  $\text{AgNO}_3$ –ChS–glucose system is completely covered with a ChS shell, with a thickness of about 1 nm, which causes the plasmon absorption spectrum to extend over the wavelength range from about 325 nm to 800 nm or more, with a surface plasmon absorption maximum around 429 nm.

### 3.3. FTIR spectroscopy

AgNPs powder was analyzed by FTIR spectroscopy to obtain valuable information about the functional groups involved in the reduction of silver ions. The use of ChS and glucose as reducing and stabilizing agents was investigated by FTIR, which

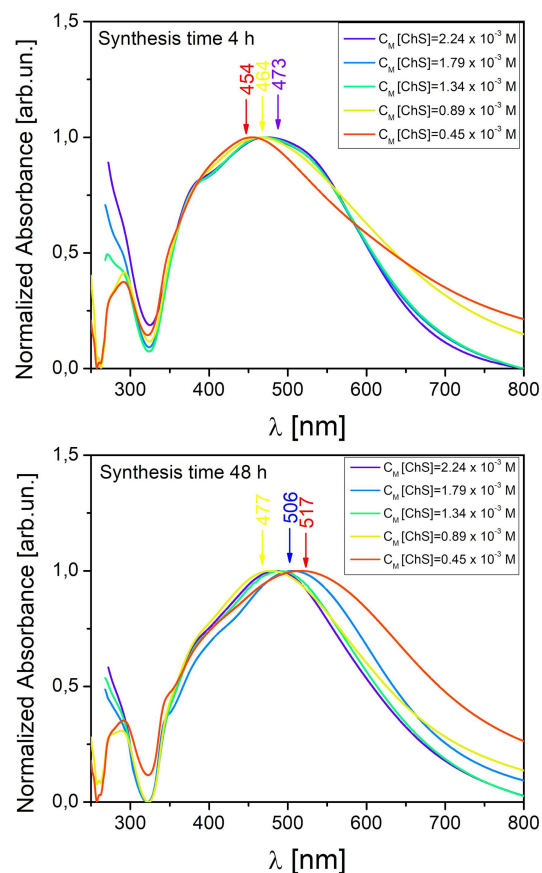


Fig. 4. UV-VIS absorption spectra of AgNPs in dependence on the synthesis time and  $C_M$  of ChS silver nanoparticles dispersed in double-distilled water for AgNPs–ChS.

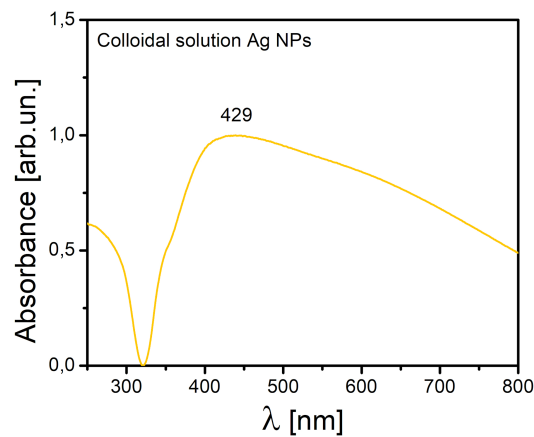


Fig. 5. UV-VIS absorption spectra of silver nanoparticles dispersed in double-distilled water for AgNPs. UV-VIS spectra reveal the formation of silver nanoparticles by surface plasmon resonance at 429 nm for AgNPs–ChS.

can help to identify the functional groups associated with these substances. FTIR spectra were recorded for  $\text{AgNO}_3$  powders, glucose, and AgNPs after reduction and ChS coating.

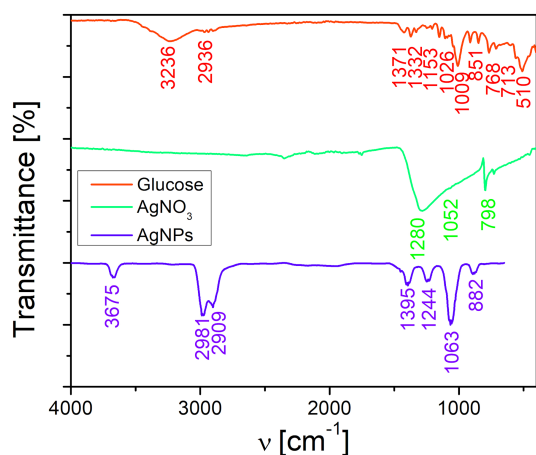


Fig. 6. FTIR spectra of  $\text{AgNO}_3$ , glucose, and AgNPs after reduction and coating with ChS.

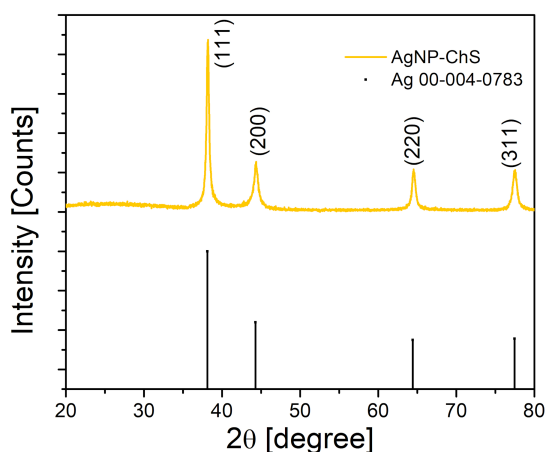


Fig. 7. XRD pattern of AgNPs–ChS.

The FTIR spectrum of  $\text{AgNO}_3$  (Fig. 6) shows characteristic bands of the nitrate group, located at 1280, 1052, and  $798\text{ cm}^{-1}$ . The band at  $1280\text{ cm}^{-1}$  is slightly shifted from the usual range for the asymmetric nitrate group stretching ( $1380\text{--}1410\text{ cm}^{-1}$ ). This difference can be attributed to the influence of crystal structure or intermolecular interactions. The band at  $1052\text{ cm}^{-1}$  falls well within the range of  $1040\text{--}1060\text{ cm}^{-1}$  for the symmetric  $\text{NO}_3^-$  group stretching. The band at  $798\text{ cm}^{-1}$  is associated with the deformation of the  $\text{NO}_3^-$  group. Comparative analysis of the bands identified in the FTIR spectra of AgNPs with those of chondroitin sulfate, glucose, and  $\text{AgNO}_3$  shows that most of the bands align well with those observed in the ligands used (chondroitin sulfate and glucose), but with some shifts, which may reflect specific interactions and structural changes caused by the synthesis of silver nanoparticles. Shifts towards higher frequencies ( $3675\text{ cm}^{-1}$ ) suggest strong interactions of hydroxyl groups with the nanoparticles. Slight shifts in the C–H bands ( $2981$  and  $2909\text{ cm}^{-1}$ ) suggest changes in the chemical environment of the

C–H groups. The good alignment of the bands for the sulfate and  $\text{NO}_3^-$  groups ( $1244\text{ cm}^{-1}$ ) suggests that functional groups are present and interact with the nanoparticles. *X-ray diffraction* (XRD) analysis confirmed the crystalline nature of the AgNPs, revealing a distinct plane shown in Fig. 7.

All the reflections correspond to pure silver metal with face-centered cubic symmetry. The intensity of peaks reflected the high degree of crystallinity of the AgNPs.

#### 4. Conclusions

In this study, a one-step “green” synthesis of AgNPs was developed. The synthesis was carried out in a stirred aqueous environment at  $T = 40^\circ\text{C}$ , using ChS as a stabilizing agent and glucose as a reducing agent. The reaction temperature, reaction time, and ChS concentration had obvious effects on the amount of AgNPs formed and the distribution of nanoparticles. Chemical reduction of silver species in a ChS–glucose– $\text{AgNO}_3$  solution at  $T = 40^\circ\text{C}$  yields monodispersed AgNPs with an average nanoparticle size of 20 nm after 48 h of release. The UV-VIS spectra indicate that the position of the surface plasmon absorption peak of the silver colloids shifts from 464 nm at 2 h of synthesis to 471 nm at 48 h of reaction. This pre-redshift of the optical spectra of AgNPs is related to an increase in particle size, a process that may involve the reduction of  $\text{Ag}^-$  adsorbed at the particle-solution interface. Comparative analysis of the bands identified in the FTIR spectra of AgNPs with those of ChS, glucose, and  $\text{AgNO}_3$  shows that most of the bands align well with those observed in the ligands used, but with some shifts, which may reflect specific interactions and structural changes caused by the synthesis of AgNPs. XRD spectroscopy confirmed the presence of elemental silver signal and no peaks of other impurities were detected. The result indicates that the synthesized product consists of high-purity AgNPs.

#### References

- [1] P. Gorelkin, N. Kalimina, A. Lov, V. Makarov, M. Tal'yanskiy, I. Yamnskiy, *Nanoindustriya* **2012**, 16 (2012).
- [2] H.M. Abuzeid, C.M. Julien, L. Zhu, A.M. Hashem, *Crystals* **13**, 1576 (2023).
- [3] A.I. Osman, Y. Zhang, M. Farghali et al., *Environ. Chem. Lett.* **22**, 841 (2024).
- [4] A. El-Badawy, D. Feldhake, *Venkatapathy State of the Science Literature Reviews Evolving Nanosilver and More*, No. 95, 2010, p. 23.

- [5] A. Pal, S. Shah, S. Devi, *Colloids Surf. A* **302**, 51 (2007).
- [6] Z. Chen, L. Gao, *Mater. Res. Bull.* **42**, 1657 (2007).
- [7] A. Kumar, H. Jochi, A. Mandole, M. Sasstry, *J. Colloid Interface Sci.* **264**, 396 (2003).
- [8] D.G. Li, S.H. Chen, S.Y. Zhao, X.M. Hou, X.G. Yang, *Thin Solid Films* **460**, 396 (2004).
- [9] G. Wang, C. Shi, N. Zhao, X. Du, *Mater. Lett.* **61**, 3795 (2007).
- [10] J.I. Mock, M. Barbic, D.R. Smith, D.A. Schultz, S. Schultz, *J. Chem. Phys.* **116**, 6775 (2002).